Thermodynamic Consequences of Bipartite Immunity Protein Binding to the Ribosomal Ribonuclease Colicin E3[†]

Daniel Walker,[‡] Geoffrey R. Moore,[§] Richard James,[||] and Colin Kleanthous*[,‡]

Department of Biology, University of York, York YO10 5YW, United Kingdom, School of Chemical Sciences, University of East Anglia, Norwich NR4 7TJ, United Kingdom, and Division of Microbiology and Infectious Diseases, University Hospital, Queens Medical Centre, University of Nottingham, Nottingham NG7 2UH, United Kingdom

Received December 17, 2002; Revised Manuscript Received February 19, 2003

ABSTRACT: Colicin E3 is a 60 kDa, multidomain protein antibiotic that targets its ribonuclease activity to an essential region of the 16S ribosomal RNA of *Escherichia coli*. To prevent suicide of the producing cell, synthesis of the toxin is accompanied by the production of a 10 kDa immunity protein (Im3) that binds strongly to the toxin and abolishes its enzymatic activity. In the present work, we study the interaction of Im3 with the isolated cytotoxic domain (E3 rRNase) and intact colicin E3 through presteady-state kinetics and thermodynamic measurements. The isolated E3 rRNase domain forms a high affinity complex with Im3 ($K_d = 10^{-12}$ M, in 200 mM NaCl at pH 7.0 and 25 °C). The interaction of Im3 with full-length colicin E3 under the same conditions is however significantly stronger ($K_d = 10^{-14}$ M). The difference in affinity arises almost wholly from a marked decrease in the dissociation rate constant for the full-length complex (8×10^{-7} s^{-1}) relative to the E3 rRNase-Im3 complex (1×10^{-4} s^{-1}), with their association rates comparable ($\sim 10^8$ M^{-1} s^{-1}). Thermodynamic measurements show that complex formation is largely enthalpy driven. In light of the recently published crystal structure of the colicin E3-Im3 complex, the additional stabilization of the wild-type complex can be ascribed to the interaction of Im3 with the N-terminal translocation domain of the toxin. These observations suggest a mechanism whereby dissociation of the immunity protein prior to translocation into the target cell is facilitated by the loss of the Im3-translocation domain interaction.

Bacteriocins are protein antibiotics produced by bacteria to gain a competitive advantage in a defined ecological niche. Bacteriocin genes or pseudo genes have been found in diverse bacteria such as *Klebsiella pneumonia*, *Yersinia pestis*, *Photorabdus luminescens*, and *Pseudomonas aeruginosa* and may be either chromosomally or plasmid encoded (*1*, *2*). Perhaps the most well-studied bacteriocin family are the plasmid encoded colicins of *Escherichia coli* that kill susceptible cells through either a nonspecific DNase activity (*3*), a highly specific RNase activity (*4*, *5*), cytoplasmic membrane depolarization (*6*), or in the case of colicin M, by the inhibition of murein synthesis (*7*).

Colicin production is directed specifically against competing *E. coli* and other closely related strains; more distantly related bacteria lack the specific import apparatus required for colicin translocation. Consequently, both the producing and the target cell possess the import apparatus required for colicins to exert their cytotoxic action. An efficient mechanism of suicide prevention is thus required to protect the producing cell from the cytotoxic effects of the colicin both on synthesis and from exogenous entry. This protection is afforded by the synthesis of a small (∼10 kDa) immunity protein that is highly specific for each colicin type (*8*). In the case of the enzymatic colicins (E2-E9, D), whose cellular targets are present in the cytoplasm, a high affinity heterodimeric complex is formed between the toxin and the immunity protein. This complex is released into the extracellular medium, and the immunity protein is jettisoned on binding of the complex to the outer-membrane receptor of susceptible cells (*9*). The high affinity nature of colicin-immunity protein interactions was originally surmised from the fact that they copurify with 1:1 stoichiometry and can only be separated under denaturing conditions (*10*). For the DNase type colicin E9, the K_d of the colicin−immunity protein interaction was subsequently determined as $\sim 10^{-14}$ M at pH 7.0 in 200 mM NaCl and 25 °C (*11*). This interaction is among the tightest protein−protein interactions reported in the literature but is comparable to other nuclease−inhibitor complexes such as those reported for barnase with its inhibitor barstar and RNase A and angiogenin with the ribonuclease inhibitor protein (RI) (*12*, *13*).

The immunity proteins of enzymatic colicins bind strongly to the nuclease domains of the toxins but at a position distant from the active site (*14*). This mode of exosite binding and inhibition is distinct to that seen in other enzyme−inhibitor complexes such as barnase−barstar (*15*, *16*) and the uracil DNA glycosylase−uracil DNA glycosylase inhibitor complex (*17*, *18*) where the inhibitor binds directly to active site residues but is observed in some protease inhibitor complexes such as the thrombin−triabin complex (*19*). A unique feature

[†] This work was supported by the UK Biotechnology and Biological Science Research Council.

* To whom correspondence should be addressed. Tel +44 (0)1904 328820. E-mail: ck11@york.ac.uk.

[‡] University of York.

[§] University of East Anglia.

[||] University of Nottingham.

10.1021/bi0273720 CCC: $25.00
Published on Web 03/22/2003

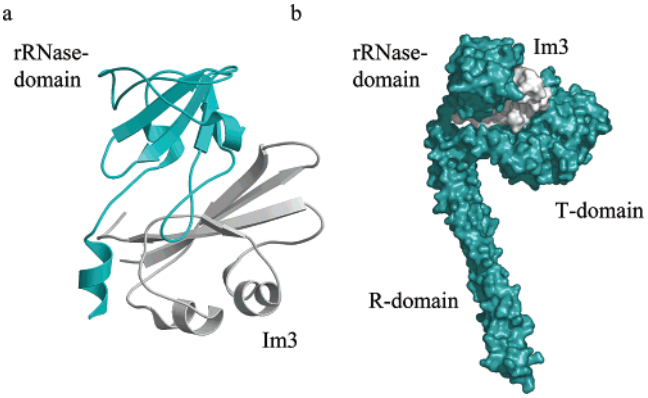

FIGURE 1: Structures of the E3 rRNase-Im3 and colicin E3-Im3 complexes. (a) Ribbon diagram of the E3 rRNase-Im3 complex (PDB code 1e44). E3 rRNase is shown in cyan and Im3 in gray. The truncated E3 rRNase-Im3 complex used for structure determination by Carr et al. (*23*) shown here is identical to that used in this work and corresponds to residues 449−551 of colicin E3. No electron density was observed for the first seven amino acids of E3 rRNase. (b) Surface representation of colicin E3-Im3 complex, with colicin E3 shown in cyan and Im3 in gray (PDB code 1jch). The colicin E3-Im3 structure shows that the toxin is highly elongated, containing a long helical hairpin, which encompasses the receptor binding domain. Both the globular rRNase and the translocation domains form substantial contacts with Im3. Approximately 40% of the accessible surface area of Im3 is lost on complex formation with colicin E3 (*24*).

of enzymatic colicin−immunity complexes is that the immunity protein binds to the most sequence variable region of the enzymatic domain. It is thought that this mode of inhibition permits the evolution of novel binding specificities in conjunction with the maintenance of the catalytic activity of the toxin (*14*). A consequence of this is the existence of families of closely related toxins, such as the DNase type colicins (E2, E7, E8, and E9) and the 16S rRNase colicins (E3, E4, and E6) that share identical catalytic activities within each family but have differing immunity specificities (*20*).

The cytotoxicity of colicin E3 is due to an RNase activity which catalyses a single, site-specific cleavage of the 16S ribosomal RNA leading to the arrest of protein synthesis (*5*, *21*). Cleavage occurs at the phosphodiester bond between bases A1493 and G1494 of the 16S rRNA. Structures of ribosomal 70S complexes containing tRNA and mRNA show that bases A1492 and A1493 interact directly with the tRNA-mRNA codon-anticodon helix at the ribosomal A site (*22*), thus revealing the critical nature of the colicin E3 cleavage site to the function of the ribosome.

The structure of the isolated E3 rRNase-Im3[1] complex (identical to that used here) has been determined by X-ray crystallography (ref *23*, Figure 1a). The protein−protein interface of the E3 rRNase-Im3 complex is significantly larger (2550 Å^2) than those of the colicin E9 DNase-Im9 (1575 Å^2) and E7 DNase-Im7 (1473 Å^2) complexes (*23*). In addition, the E3 rRNase-Im3 complex also differs in the degree of hydrophobic burial and number of water molecules buried at the interface as compared to DNase-Im protein complexes. It was therefore of considerable interest to determine and compare the kinetics, thermodynamics, and mechanism of complex formation of the E3 rRNase-Im3 complex both with those of other colicin cytotoxic domain−immunity protein complexes and other nuclease−inhibitor complexes. During the course of this work, a structure of the full-length colicin E3-Im3 complex was described (*24*). This revealed that in addition to the E3 rRNase-Im3 interface the immunity protein also forms a significant interface with the translocation domain (ref *24*, Figure 1b). We have therefore also investigated the interaction of Im3 with intact, full-length colicin E3 to determine if this additional interaction is of thermodynamic and physiological significance to the colicin E3-Im3 complex. Through this comparison, we propose a mechanism by which the tightly bound immunity protein is able to dissociate from the colicin during translocation of the toxin into a target cell.

MATERIALS AND METHODS

Bacterial Strains and Media. E. coli strain JM83 was used as the host strain for initial cloning of recombinant pUC and pET vectors, for the overexpression of the full length colicin E3-Im3 complex (containing the plasmid pColE3) and for the assessment of colicin cytotoxic activity (containing the plasmid pTrc99a). BL21(DE3) was used for IPTG induced protein expression from recombinant pET21 based plasmids. The methionine auxotroph B843(DE3) was used for L-[methyl-^{3}H]methionine labeling of Im3. Cultures were grown in LB broth or on plates of LB agar, supplemented where necessary with ampicillin (100 μg/mL) or chloramphenicol (35 μg/mL). X-gal (40 μg/mL) was used on LB agar plates for the chromogenic selection of recombinant pUC18 plasmids.

Plasmid Construction. PCR was used to amplify a 1933 base pair *Nde*I-*Xho*I fragment, coding for the colicin E3 structural genes from the ColE3-CA38 plasmid (*25*). The purified DNA was blunt-ended and cloned into the *Sma*I site of pUC18, transformed into JM83, and grown on LB agar containing X-gal allowing for the chromogenic selection of recombinant plasmids. Digestion of recombinant plasmids with *Nde*I and *Xho*I and cloning of the excised fragment into pET21a (Novagen) gave the plasmid pRJ382. pDW1, used for the tandem overexpression of the E3 rRNase-Im3(His$_6$) complex was constructed similarly using pRJ382 as the template for PCR and pET21d (Novagen) as the expression vector. An *Nco*I site was introduced six amino acids upstream of the previously identified enzymatically active, so-called T2A fragment of colicin E3 (*10*), herein referred to as the E3 rRNase domain, and an *Xho*I site was introduced in place of the stop codon of Im3. pDW2, used for the overexpression of wild-type Im3, was constructed as above by the introduction of *Nco*I and *Xho*I sites at the start and stop codons of the Im3 gene, respectively.

Protein Purification. E3 rRNase was purified essentially as described for the E9 DNase (*26*). Briefly, the E3 rRNase-Im3 complex was tandemly expressed, and the complex was isolated by nickel affinity chromatography through an engineered six histidine tag located at the C-terminus of Im3. E3 rRNase was eluted from the column by denaturation of the complex in 6 M guanidine hydrochloride, and the isolated

[1] Abbreviations: E3 rRNase, 16S ribosomal RNA specific ribonuclease domain of colicin E3; Im3, immunity protein of colicin E3; T-domain, colicin translocation domain; R-domain, colicin receptor binding domain; E9 DNase, the endonuclease domain of colicin E9; IPTG, isopropyl-β-D-thiogalactopyranoside; X-gal, 5-bromo-4-chloro-3-indolyl β-D-galactopyranoside; MOPS, 3-[*N*-morpholino]propanesulfonic acid; k_{obs}, observed rate constant; k_{on}, bimolecular association rate constant; k_{off}, dissociation rate constant.

rRNase was refolded by extensive dialysis into water followed by 50 mM KPi, pH 7.0. A final gel filtration step (Superdex-75) in 50 mM KPi, pH 7.0, was used to remove any remaining contaminants. Electrospray ionization mass spectrometry (Micromass Platform), performed under the conditions described by Wallis et al. (*27*), gave a mass of 11 799.0 Da for E3 rRNase, close to the expected mass of 11 800.3 Da.

Im3 was expressed from *E. coli* strain BL21 (DE3) harboring the plasmid pDW2 and purified essentially as described for Im9 (*28*) with minor modifications. The mass of purified Im3, determined by ESI−MS, was 9773.5 Da, which corresponds to the expected mass minus the N-terminal methionine (9772.6 Da). L-[methyl-^{3}H]methionine labeled Im3, for radioactive subunit exchange experiments, was purified from a culture of the methionine auxotroph B843 (DE3), harboring the plasmid pDW2. The specific radioactivity of the purified protein was determined as 3.3 μCi/μmol Im3 by liquid scintillation counting, using an LBK 1214 RACKBETA liquid scintillation counter (Wallac).

The colicin E3-Im3 complex was purified by the same method described by Wallis et al. (*28*) for the purification of the colicin E9-Im9 complex. Free colicin E3 was isolated by denaturation of the colicin E3-Im3 complex in 50 mM potassium phosphate, pH 7.0 containing 5 M guanidine hydrochloride and separated on a preparative Superdex S75 column (Pharmacia) equilibrated in the same buffer. Free colicin E3 (referred to as E3* by other authors) was refolded by dialysis into 50 mM potassium phosphate, pH 7.0.

Protein Estimation. Protein concentrations were routinely measured from the absorbance at 280 nm using a Philips PU8730 spectrophotometer. Extinction coefficients ($\epsilon^{0.1\%}$ mL mg^{-1} cm^{-1}) of 1.67 and 2.22 were determined for purified E3 rRNase and Im3, respectively, based on amino acid analysis data (Alta Bioscience). Concentrations of free colicin E3 and the colicin E3-Im3 complex were based on previously reported $\epsilon^{0.1\%}$ values of 1.10 and 1.24, respectively (*29*).

Tryptophan Fluorescence Emission Experiments. Static fluorescence measurements of intrinsic tryptophan fluorescence were performed on a Spex FluoroMax-3 spectrofluorimeter using an excitation wavelength of 295 nm with excitation and emission slit widths set at 3 nm. Fluorescence emission spectra were collected from 300 to 400 nm.

Stopped-flow fluorescence experiments were performed on an Applied Photophysics Bio-Sequential Stopped-flow Spectrofluorimeter set up for 1:1 single mixing. An excitation wavelength of 280 nm was used in all experiments. Fluorescence was monitored above 305 nm; fluorescence of a shorter wavelength was excluded using a 305 nm cutoff filter. The manual entrance and exit slits were set to 0.7 mm. Experiments were carried out in 50 mM MOPS, 1 mM DTT, pH 7.0, with added NaCl in the range of 100−500 mM where indicated and at 25 °C unless otherwise stated. A total of 4000 data points were collected over the course of each reaction, and data from 10 runs were averaged for each measurement. Data collected before 2 ms were not included in the analysis.

The association of E3 rRNase and Im3 was monitored under both pseudo-first-order and second-order conditions. In the former case, the Im3 concentration was kept constant (0.32 μM, 0.05 μM, or 5 nM) with the E3 rRNase concentration varied as stated in the text. Data were fitted to a single-exponential rate equation. Pseudo-first-order plots of k_{obs} against E3 rRNase concentration, which were linear in all cases, were used to determine the bimolecular association rate (k_{on}). Second-order experiments, used to determine bimolecular association rates at varying salt concentrations, were conducted at identical E3 rRNase and Im3 concentrations (0.05 or 0.32 μM), and the data were fitted to eq 1

$$F = F_0 + \Delta F[E]_0 k_{on} t/(1 + [E]_0 k_{on} t) \quad (1)$$

where F_0 is the fluorescence at time $t = 0$, F is the fluorescence at time t, $[E]_0$ is the initial protein concentration of one of the components, and ΔF is the total change in fluorescence (*12*). The bimolecular association rate k_{on} was determined directly from this fit.

Radiolabeled Subunit Exchange. Radiolabeled subunit exchange experiments were performed to determine the dissociation rates of the E3 rRNase-Im3 and colicin E3-Im3 complexes. Experiments were conducted in 50 mM MOPS, 1 mM DTT, pH 7.0 with added NaCl where required. Either unlabeled Im3 (50 μM) was used to exchange with [^{3}H]Im3 from a preformed E3 rRNase-[^{3}H]Im3 complex (5 μM) or labeled [^{3}H]Im3 (50 μM) was exchanged into a preformed unlabeled E3 rRNase-Im3 complex (5 μM). The E3 rRNase-Im3 complex was separated from unbound Im3 using a Mono Q anion exchange column (HR 5/5, Pharmacia Biotech) equilibrated in 50 mM Tris-HCl, pH 7.0. 100 μL of sample was loaded onto the column, and separation of the components was achieved using a 0−1 M NaCl gradient. Fractions from the complex and free Im3 peaks were counted for 5 min on an LBK 1214 RACKBETA liquid scintillation counter (Wallac). The percent exchange was calculated from the ratio of the disintegrations per minute (dpm) counted in the complex peak to the dpm counted for both peaks after correction for background counts, and the data were fitted to a single-exponential rate equation. Exchange experiments for the colicin E3-Im3 complex were performed similarly except separation of the complex from free immunity protein was performed on an S75 HR10/30 gel filtration column (Pharmacia) equilibrated in 50 mM KPi, pH 7.0.

In vitro E3 rRNase Activity Assays. The activity of free colicin E3 rRNase directed against *E. coli* ribosomes was ascertained through an in vitro transcription/translation assay using the *E. coli* T7 S30 extract system for circular DNA (Promega). The activity of E3 rRNase was determined by the presence or absence of a reporter protein (chloramphenicol acetyl transferase) encoded by the Pinpoint Control Vector (Promega), the absence of the reporter protein indicating ribosome inactivation and E3 rRNase activity. Components of the transcription/translation system were set up according to the manufacturer's instructions using 20 μL of S30 premix, 15 μL of T7 30S extract, 5 μL of amino acid mixture minus methionine, and 1 μL of [^{35}S]methionine (1200 Ci/mmol, Amersham) per assay. E3 rRNase (at the required concentration in 50 mM Tris-HCl, pH 7.0) was added to the S30 mix and incubated for 10 min at 37 °C, prior to the addition of 1 μg of the Pinpoint DNA template. The reactions were then incubated for a further hour at 37 °C, and 5 μL of the mixture was loaded onto a 15% SDS polyacrylamide gel. Bands were visualized by exposing a Kodak SO-230 phosphor storage screen to the dried gel for

4 h and measuring phosphorescence on a Storm 840 phosphoimager (Molecular Dynamics).

Isothermal Titration Calorimetry (ITC). ITC experiments were performed on a VP−ITC microcalorimeter (MicroCal, LLC) in 50 mM MOPS, 200 mM NaCl, pH 7.0 at 25 °C with E3 rRNase (20 μM) in the cell (cell volume = 1.4285 mL) and Im3 (312 μM) in the syringe. Im3 was titrated into E3 rRNase using an initial injection of 2 μL followed by 34 × 7 μL injections with stirring at 300 rpm. Proteins were dialyzed overnight prior to ITC measurements into the dialysis buffer used for protein heat of dilution control experiments. Data for E3 rRNase-Im3 complex formation were fitted to a single site binding equation after correction for heat of dilution of using MicroCal ORIGIN software.

Sedimentation Equilibrium. Sedimentation equilibrium runs were performed using a Beckman Optima XL-I. Samples of E3* and the colicin E3-Im3 complex were equilibrated in 50 mM KPi, 200 mM NaCl, pH 7.0 by gel filtration (Superdex-75, HR10/30, Pharmacia). Each protein sample (110 μL) and a buffer reference sample (116 μL) were loaded into double sector, charcoal filled Epon cells of 12 mm optical path length. Experiments were performed at 20 °C at a rotor speed of either 10 000 or 15 000 rpm, where specified, using an AN-50Ti rotor. Data were acquired at 280 nm, and analysis was performed using the software provided by Beckman, using values of 0.7224 mL/g for the partial specific volume of the protein and 1.014 g/mL for the solvent density. The data were fitted to the Lamm equation (eq 2) for a single ideal species

$$c_r = c_{r_0} \exp[\omega^2 M(1 - \bar{v}\rho)(r^2 - r_0^2)/2RT] \qquad (2)$$

where c_r is the concentration at radius r, c_{r_0} is the concentration of the monomer at reference radius r_0, ω is the angular velocity, R is the gas constant, T is the temperature (K), M is the monomer molecular weight, $\bar{v}$ is the partial specific volume of the protein, and ρ is the solvent density (*30*).

RESULTS

Refolded E3 rRNase Is Both Enzymatically Active and Functional in Immunity Protein Binding. The rRNase activity of colicin E3 is directed against the 16S ribosomal RNA, with cleavage resulting in the loss of around 50 bases from its 3′ end and the inactivation of the ribosome (*5*). Colicin E3 activity can therefore be monitored either by the reduction in size of the 16S rRNA or by the ability of E3 treated ribosomes to support protein synthesis (*31*). Uncomplexed E3 rRNase used in the present study was obtained by isolating the E3 rRNase-Im3(His_6) complex by metal chelation chromatography, eluting the E3 rRNase under denaturing conditions with 6 M guanidine hydrochloride, and then refolding the rRNase by dialysis into water. The functionality of refolded E3 rRNase therefore needed to be evaluated for catalytic activity (directed against bacterial ribosomes) and the ability of its cognate immunity protein, Im3, to inhibit this activity. E3 rRNase catalytic activity was assessed through an in vitro transcription−translation assay by monitoring the incorporation of ^{35}S methionine into a reporter protein (see Materials and Methods). By this method, refolded E3 rRNase was found to inactivate *E. coli* ribosomes at concentrations in excess of 10 nM, a value similar to that previously reported for colicin E3 in vitro activity (*10*). Importantly, this activity was abolished by the addition of a stoichiometric amount of Im3 (Figure 2). Refolded E3 rRNase is thus both enzymatically active and functional in immunity protein binding.

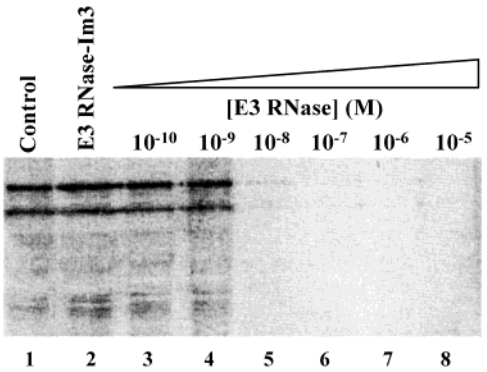

FIGURE 2: In vitro transcription translation assay demonstrating inactivation of the ribosome by E3 rRNase and inhibition of E3 rRNase activity by Im3 (see Materials and Methods). E3 rRNase activity leading to ribosome inactivation and the abolition of protein synthesis was determined by the absence of [^{35}S] labeled protein on the gel. Inactivation of ribosomes is observed at E3 rRNase concentrations down to approximately 10^{-8} M (lanes 3−8). Addition of Im3 to the isolated E3 rRNase (10^{-6} M complex, lane 2) completely abolished catalytic activity.

E3 rRNase-Im3 Complex Formation Monitored by Intrinsic Tryptophan Fluorescence. The formation of protein−protein complexes can often give rise to a significant change in the magnitude and/or wavelength of the intrinsic tryptophan fluorescence relative to the component proteins, which has proved to be a useful tool in the study of nuclease−inhibitor interactions (*11*, *12*, *20*). We found that the formation of the E3 rRNase-Im3 complex is accompanied by a substantial enhancement in the intrinsic tryptophan fluorescence relative to the component proteins (Figure 3a). At the λ_{max} of the complex, the enhancement in fluorescence is approximately 50% over the isolated proteins. Figure 3b shows the results of a titration of Im3 into a solution of E3 rRNase. An initial linear enhancement up to a stoichiometry of 1:1 is observed followed by a further enhancement equivalent to adding Im3 to buffer (Figure 3b). The linear enhancement in fluorescence observed on complex formation indicates that the equilibrium dissociation constant is too small to determine by this method. For such complexes, an alternative route to the determination of the K_d is to calculate the association and dissociation rate constants, from which the K_d can then be calculated from the ratio of k_{off}/k_{on} (*12*).

Determination of the Association Rate Constant for the E3 rRNase-Im3 Complex. The large enhancement in intrinsic tryptophan fluorescence on formation of the E3 rRNase-Im3 complex was used to follow the rate of complex formation by stopped-flow fluorescence. Association was monitored under both second-order and pseudo-first-order conditions. Under pseudo-first-order conditions with either Im3 or E3 rRNase in excess, the data were well-described by a single-exponential rate equation, with no obvious trend in the residuals of the fit (Figure 4a). The observed rate under pseudo-first-order conditions is independent of which component is in excess as would be expected if a single process is being monitored. Pseudo-first-order plots, with either E3 rRNase or Im3 at a concentration of 0.05 μM and the other

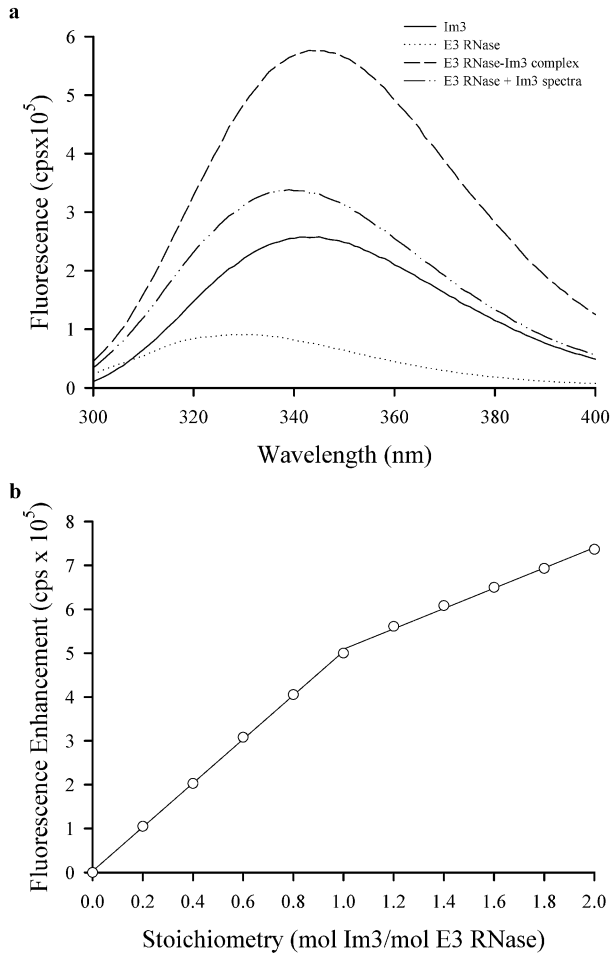

FIGURE 3: Formation of the E3 rRNase-Im3 complex gives rise to a large increase in the intrinsic tryptophan fluorescence over the component proteins. (a) Fluorescence emission spectra of E3 rRNase and Im3 and the E3 rRNase-Im3 complex were recorded at a protein concentration of 0.5 μM in 50 mM MOPS, 200 mM NaCl, pH 7.0. The spectra obtained after adding the spectra of E3 rRNase and Im3 together is also shown for comparison (E3 rRNase + Im3). (b) Stoichiometry of complex formation monitored by titrating Im3 into a solution of E3 rRNase. A linear enhancement in the intrinsic tryptophan fluorescence on E3 rRNase-Im3 complex formation is observed up to a molar ratio of 1:1. The addition of further Im3 to this solution increases the measured fluorescence by the same amount as adding Im3 to buffer (data not shown).

component in a 6−30-fold excess, are linear, with the intercept very close to zero indicating a slow dissociation rate that cannot be accurately estimated from this plot (Figure 4b). A bimolecular association rate of 1.1(±0.1) × 10^8 M^{-1} s^{-1} (in 50 mM MOPS, 200 mM NaCl at pH 7.0) was obtained from the pseudo-first-order plot. Additional experiments with Im3 at a concentration of 0.32 μM and E3 rRNase in a 6−16-fold excess yielded essentially identical results (data not shown). Under second-order conditions, data were accurately described by a simple second-order equation (*12*) indicating that a single association step is indeed being monitored in the stopped-flow experiment (data not shown). Using protein concentrations of 50 nM in 50 mM MOPS, 200 mM NaCl at pH 7.0, a rate of 1.1(±0.0) × 10^8 M^{-1} s^{-1} was obtained for the bimolecular association rate constant, identical to that observed under pseudo-first-order conditions. Fast diffusion-controlled association reactions have been observed for many nuclease−inhibitor complexes, such as barnase−barstar and colicin E9 DNase-Im9 (*11*, *12*). In these

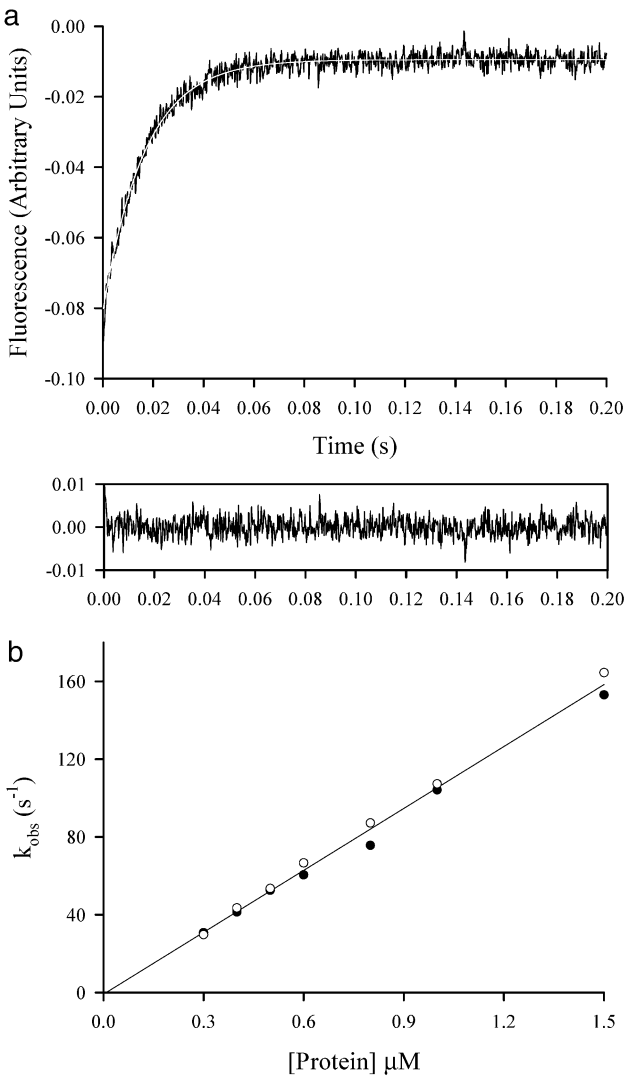

FIGURE 4: Association of E3 rRNase with Im3 monitored by stopped-flow tryptophan fluorescence under pseudo-first-order conditions. Either E3 rRNase or Im3 was kept at a constant concentration (0.05 μM) throughout the experiment with the concentration of the other protein present in a 6−30-fold excess. (a) Example stopped-flow fluorescence trace monitoring the association of E3 rRNase (0.05 μM) and Im3 (0.6 μM) in 50 mM MOPS, 200 mM NaCl, pH 7.0 at 25 °C. The fit to a single-exponential rate equation is shown in gray (k_{obs} = 61 s^{-1}), and the residuals to this fit are shown in the lower panel. (b) Plot of k_{obs} against protein concentration for E3 rRNase (○) or Im3 (●) in excess. The fit to the data was obtained by linear regression, and the bimolecular association rate constant k_{on} was calculated from the slope of the line (k_{on} = 1.1 × 10^8 M^{-1} s^{-1}). The intercept of the fitted line at zero protein concentration has a value very close to zero (−0.8 s^{-1}).

cases, as with the E3 rRNase-Im3 complex, the rate of association is close to the theoretical diffusion controlled limit of 7 × 10^9 M^{-1} s^{-1}, calculated for uncharged, uniformly reactive spheres (*32*). The association rate constants of most protein−protein complexes are many orders of magnitude lower than this since the protein surface is far from uniformly reactive, the combining sites representing only a small proportion of each protein's accessible surface area. However, the formation of protein−protein complexes with association rate constants in excess of this limit are possible and are generally indicative of strong, favorable electrostatic interactions that preorient the proteins before collision (*11*, *12*, *33*, *34*). To address this issue in the E3 rRNase-Im3

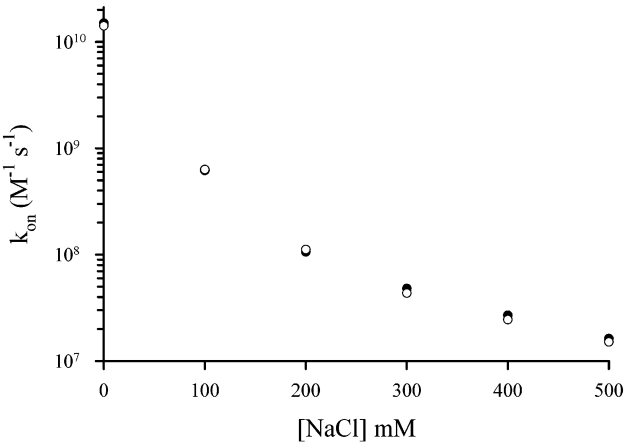

FIGURE 5: Salt dependence of the bimolecular association rate constant for the E3 rRNase-Im3 complex. Plot of k_{on} against NaCl concentration for the association of E3 rRNase and Im3. Experiments performed at 0.05 μM (●) and 0.32 μM (○) protein concentrations.

Table 1: Calculated Activation Parameters for the E3 RNase-Im3 Complex[a]

rate constant	$\Delta H^{\ddagger}$ (kcal mol^{-1})	$T\Delta S^{\ddagger}$ (kcal mol^{-1})	$\Delta G^{\ddagger}$ (kcal mol^{-1})
k_{on}	5.6	0.1	5.5
k_{off}	22.3	−0.3	22.6

[a] Values were determined in 50 mM MOPS, 200 mM NaCl, pH 7.0 at 25 °C.

complex, we measured the bimolecular association rate at salt concentrations in the range of 0−500 mM NaCl (Figure 5). The bimolecular association rate constant was found to vary by approximately 3 orders of magnitude over this range, decreasing from 1.5(±0.1) × 10^{10} M^{-1} s^{-1} with no added salt to 1.6 (±0.1) × 10^{7} M^{-1} s^{-1} in 500 mM NaCl. The strong salt dependence and very fast rates of association in the absence of added salt show that electrostatic steering plays a role in the bimolecular association kinetics of the E3 rRNase-Im3 complex.

The temperature dependence of the association rate constant of protein−protein complexes can be used to determine the thermodynamic activation parameters of complex formation (*35*). The bimolecular association rate of E3 rRNase-Im3 complex formation was measured under pseudo-first-order conditions in the temperature range of 15−40 °C in 50 mM MOPS, 200 mM NaCl at pH 7.0 (data not shown). Values for the enthalpic and entropic activation parameters $\Delta H^{\ddagger}$ and $T\Delta S^{\ddagger}$ were obtained from Arrhenius plots (Table 1). The low value of $\Delta H^{\ddagger}$ and a value of $T\Delta S^{\ddagger}$ close to zero is also seen in the association of the barnase−barstar complex ($\Delta H^{\ddagger} = 5.7$ kcal mol^{-1} and $T\Delta S^{\ddagger} = -0.9$ kcal mol^{-1} at pH 8.0, 0.15 mM NaCl, and 298 K (*36*). A low enthalpic barrier is characteristic of diffusion-controlled associations and seems to be an important regulatory characteristic of nuclease−inhibitor complexes where the nuclease is potentially lethal (*37*).

Determination of the Dissociation Rate of the E3 rRNase-Im3 Complex by Radiolabeled Subunit Exchange. The dissociation rate constant (k_{off}) for the E3 rRNase-Im3 complex was determined by radiolabeled subunit exchange. Unlabeled or labeled E3 rRNase-Im3 or E3 rRNase-[^{3}H]Im3 complexes were incubated with a 10-fold excess of [^{3}H]Im3 or unlabeled Im3, respectively. The observed dissociation rate, obtained from measuring the relative amounts of complexed and uncomplexed [^{3}H]Im3 with time, after chromatographic separation, were found to be independent of which way the experiment was conducted. A value of 1.5(±0.1) × 10^{-4} s^{-1} was obtained for k_{off} in 50 mM MOPS, 200 mM NaCl at pH 7.0 and 25 °C (Figure 6). The value of k_{off} varies little with salt concentration with values of 1.8 × 10^{-4} and 2.4 × 10^{-4} s^{-1} obtained in 300 and 500 mM NaCl, respectively.

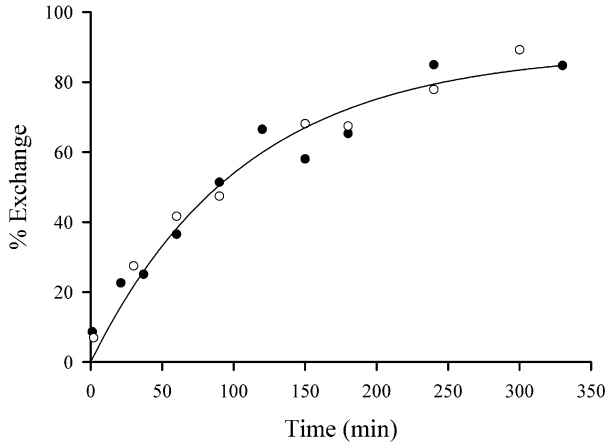

FIGURE 6: Determination of the dissociation rate constant for the E3 rRNase-Im3 complex. k_{off} was measured by radiolabeled subunit exchange in 50 mM MOPS, 200 mM NaCl, pH 7.0. The open and closed symbols represent data, from two independent experiments fitted to a single-exponential rate equation of the form $y = a(1 - e^{-kt})$.

The response of the dissociation rate to temperature was also investigated in the temperature range of 15−40 °C. Over this temperature range, k_{off} increases from 4.5 × 10^{-5} s^{-1} at 15 °C to 1.6 × 10^{-3} s^{-1} at 40 °C. At 25 °C, the half-life ($t_{1/2}$) of complex dissociation is ∼70 min but reduces to ∼8 min at 40 °C. The thermodynamic activation parameters determined for k_{off} are shown in Table 1. The importance of this change in complex dissociation rate at elevated temperatures is developed in the Discussion.

Thermodynamic Contributions to E3 rRNase-Im3 Complex Formation. The K_d for the E3 rRNase-Im3 complex can be determined directly from the ratio of k_{off}/k_{on} (*11*, *12*). In 50 mM MOPS, 200 mM NaCl at pH 7.0 and 25 °C, the K_d for the E3 rRNase-Im3 complex is 1.4(±0.1) × 10^{-12} M. This equates to a change in free energy (ΔG) of −16 kcal mol^{-1} on complex formation. In contrast to immunity protein binding to the cytotoxic domains of colicins E9 and E2 (DNase type colicins), which have K_ds of approximately 10^{-14} M under the same conditions as presented here, the K_d of the E3 rRNase-Im3 complex is relatively modest at 10^{-12} M. Values for k_{on} and k_{off} for the E3 rRNase-Im3 complex were determined, and K_d values were calculated at 15, 25, 30, and 35 °C. Over the temperature range of 15−35 °C, ΔG remains almost constant, varying by less than 0.1 kcal mol^{-1}. The contribution of ΔH over this temperature range was estimated using the van't Hoff equation $d\ln K_a/d(1/T) = -\Delta H/R$ (Figure 7a). At 298 K, the enthalpy of complex formation was estimated to be −16 kcal mol^{-1}. However, since the van't Hoff equation assumes the enthalpy change remains constant over the temperature range studied, this value can be in error. A direct measurement of the

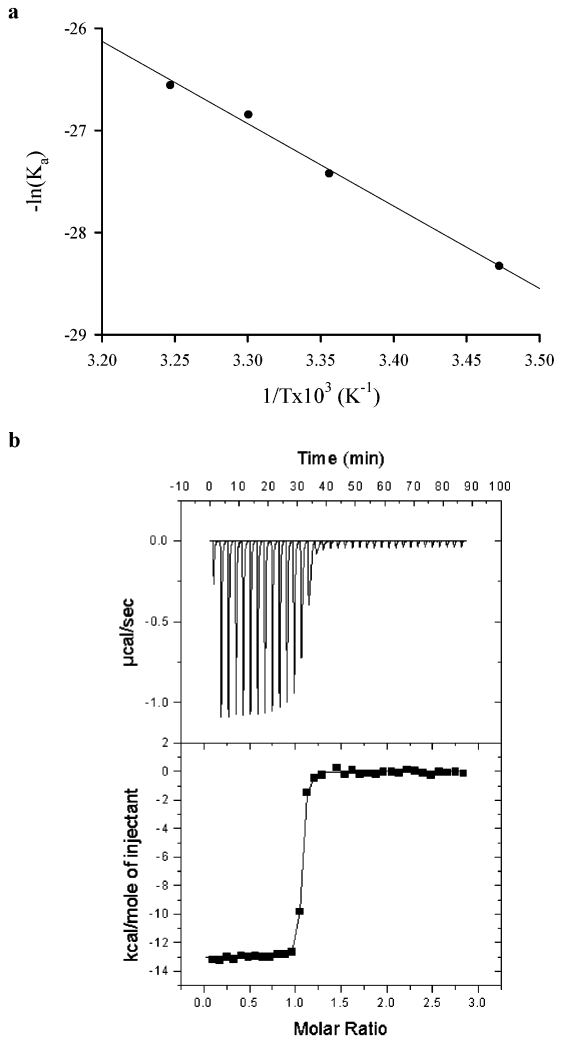

FIGURE 7: (a) van't Hoff plot for the E3 rRNase-Im3 complex. Data used in this plot are from the calculation of K_a at 15, 25, 30, and 35 °C. Experiments were performed in 50 mM MOPS, 200 mM NaCl, pH 7.0. (b) ITC data for E3 rRNase-Im3 complex formation. Experiments were performed as described in Materials and Methods. A value of -13.1 kcal mol^{-1} for ΔH and a stoichiometry of binding of 1.04 were obtained from the fit. The K_d of the complex is too low to accurately determine directly from the fit.

enthalpy change associated with the complex formation was however obtained by isothermal titration calorimetry (ITC) (Figure 7b). This gave a value for ΔH of -13 kcal mol^{-1} for the formation of the E3 rRNase-Im3 complex in 50 mM MOPS, 200 mM NaCl, pH 7.0 at 25 °C, close to that estimated from the van't Hoff equation. Formation of the E3 rRNase-Im3 complex is therefore almost entirely enthalpically driven under these conditions.

Kinetics and Thermodynamics of Colicin E3-Im3 Complex Formation. Publication of the full-length colicin E3-Im3 structure indicated that there are contacts between the immunity protein and the translocation domain in addition to those made with the rRNase domain (Figure 1b). To assess the contribution of these additional contacts to the stability of the colicin E3-Im3 complex, we performed similar kinetic experiments on the full-length complex to those performed on the E3 rRNase-Im3 complex. These experiments required uncomplexed colicin E3 that can only be obtained by separation of the colicin from the immunity protein under denaturing conditions. However, previous studies by Levinson et al. (*29*) using small-angle X-ray scattering had suggested that although the colicin E3-Im3 complex is monomeric, removal of the immunity protein leads to dimerization of the toxin, a potential problem for kinetic and thermodynamic measurements. Moreover, these studies also indicated that the addition of Im3 back to the free toxin did not result in the formation of the native colicin E3-Im3 complex. The experiments described by Levinson et al. involved very high protein concentrations (50−250 μM). In addition, the X-ray structure solved for the intact colicin E3-Im3 complex was refined as a dimer, although no functional significance has been assigned to the dimeric complex (*24*). To resolve the uncertainty regarding the oligomeric state of both free colicin E3 and colicin E3-Im3 complex in solution (prepared as described in Materials and Methods), sedimentation equilibrium experiments were performed.

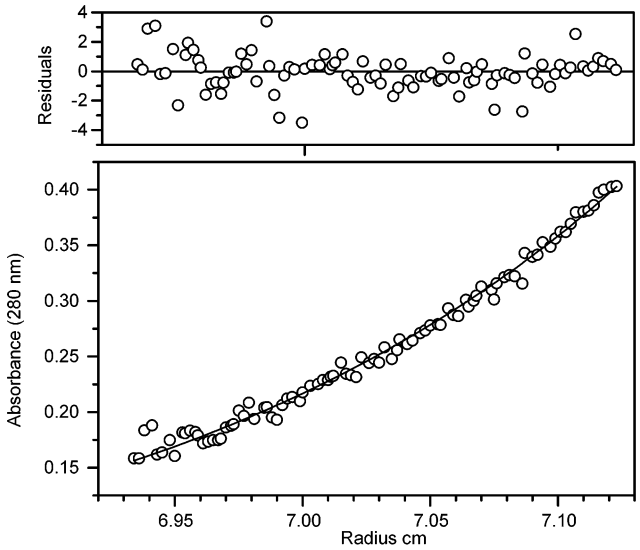

FIGURE 8: Plot of absorbance against radial distance, and the corresponding fit to a model for a single ideal species, of sedimentation equilibrium data for free colicin E3. The plot shown is for free colicin E3 at 5 μM in 50 mM KPi, 200 mM NaCl, pH 7.0. Experiments were performed on a Beckman Optima XL-I analytical ultracentrifuge at a rotor speed of 15 000 rpm, using an AN-50Ti rotor at 20 °C. Data were acquired at 280 nm and analyzed using the software provided by Beckman. The bottom panel shows a plot of A_{280} against radial distance. The collected data and the fit to the data from the Lamm equation are shown (see Materials and Methods). The plot of residuals (top panel) shows no systematic trends indicating the data fits well to the proposed model.

Sedimentation equilibrium experiments on uncomplexed colicin E3 were performed at two rotor speeds and protein concentrations of 2.5 and 5.0 μM in 50 mM KPi, 200 mM NaCl at pH 7.0 (Figure 8). An average molecular weight of 58.1($\pm$0.8) kDa ($n = 4$) was obtained, identical to the monomeric molecular weight of colicin E3 (58.1 kDa). Thus, at least at these protein concentrations, uncomplexed colicin E3 is monomeric in solution. As expected, and in accordance with the work of Levinson et al., the colicin E3-Im3 complex was also found to be monomeric. An observed weight averaged molecular weight of 74 kDa close to the actual molecular weight of 68 kDa for the complex was obtained from a single sedimentation equilibrium experiment (data not shown).

The bimolecular association rate of the full-length colicin E3 and Im3 was determined by stopped-flow fluorescence under pseudo-first-order conditions as described for the

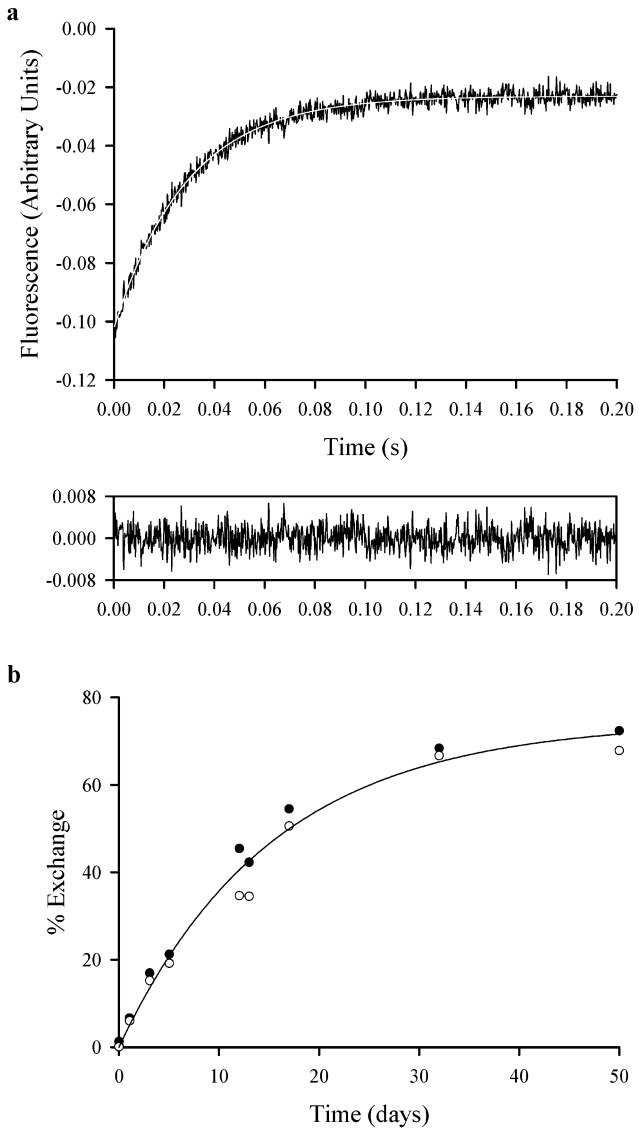

FIGURE 9: Determination of the association and dissociation rate constants for the colicin E3-Im3 complex. (a) Example stopped-flow fluorescence trace monitoring the association of E3* (0.05 μM) and Im3 (0.6 μM) in 50 mM MOPS, 200 mM NaCl, pH 7.0 at 25 °C. The fit to a single-exponential rate equation is shown in gray ($k_{obs} = 35\ s^{-1}$), and the residuals to this fit are shown in the lower panel. (b) Determination of the dissociation rate constant for the colicin E3-Im3 complex. k_{off} was measured by radiolabeled subunit exchange in 50 mM MOPS, 200 mM NaCl, pH 7.0 with 0.05% sodium azide at a colicin E3-Im3 concentration of 5 μM with a 10-fold excess of [^{3}H]Im3. The data presented are from two independent determinations run over the course of 50 days. Because of the length of time over which the experiments were required to run, fresh sodium azide and DTT were added every 7 days. The data shown, from two independent experiments, is fitted to a single-exponential rate equation of the form $y = a(1 - e^{-kt})$.

isolated domain (Figure 9a). Under these conditions, with either Im3 or colicin E3 in excess, the data were well-described by a single-exponential rate equation, indicating that a single step is being monitored in the stopped-flow experiment (Figure 9a). Pseudo-first-order plots indicated that the observed rate shows a linear concentration dependence that is independent of which component is in excess (data not shown). From this plot, a bimolecular association rate constant for the colicin E3-Im3 complex was calculated to be $5.5(\pm0.1) \times 10^7\ M^{-1}\ s^{-1}$. This value is slightly lower than for the E3 rRNase-Im3 complex, which may reflect the close proximity of the translocation domain to the catalytic domain in the intact toxin, preventing ready access of Im3 to its binding site. In contrast, the dissociation rate constant for the colicin E3-Im3 complex was found to be much lower than for the E3 rRNase-Im3 complex. A value of $7.6(\pm0.2) \times 10^{-7}\ s^{-1}$ was determined by radiolabeled subunit exchange experiments (Figure 9b), approximately 2 orders of magnitude slower than for the isolated domain complex with Im3. Hence, the K_d for the colicin E3-Im3 complex, determined from the ratio k_{on}/k_{off}, was calculated to be $1.4(\pm0.1) \times 10^{-14}\ M^{-1}\ s^{-1}$, 2 orders of magnitude tighter than for the E3 rRNase-Im3 complex (Table 2).

DISCUSSION

Colicin E3 was the first of the bacteriocins for which a specific immunity protein was identified, thus revealing the mechanism through which producing cells are able to protect themselves from the lethal effects of this class of toxins. The need to denature the colicin E3-Im3 complex to prepare free, uncomplexed colicin E3 made it apparent that the complex is of a high affinity (*31*). Later, the small and highly basic C-terminal domain was identified as housing both the specific anti-ribosomal enzymatic activity and the immunity protein binding region of the toxin (*10*). More recently, structures of the E3 rRNase-Im3 (*23*) and the full-length colicin E3-Im3 (*24*) complexes have revealed the molecular basis for both the strong E3 rRNase-Im3 interaction and the overall architecture of the colicin E3-Im3 complex, including the formation of a significant interface between the immunity and the translocation domain. In this work, we report a kinetic and thermodynamic study of the interaction of the immunity protein Im3 with the isolated E3 rRNase domain and also with full-length colicin E3.

Comparison of the Kinetics and Thermodynamics of E3 rRNase-Im3 Complex Formation with Other Nuclease−Inhibitor Complexes. Kinetic experiments show that association of Im3 with the E3 rRNase domain is essentially diffusion controlled ($\sim10^8\ M^{-1}\ s^{-1}$) and that dissociation of the resulting complex is slow ($\sim10^{-4}\ s^{-1}$). The equilibrium dissociation constant determined from these studies ($\sim10^{-12}$ M) shows that as expected a tightly bound complex is formed between E3 rRNase and Im3. Thermodynamic data indicate that this is due to a large and favorable change in enthalpy on complex formation with a small entropic contribution to give an overall free energy change on complex formation of -16.2 kcal mol^{-1}. A favorable enthalpic change is not unexpected from analysis of the E3 rRNase-Im3 structure since 15 intermolecular hydrogen bonds are formed at the protein−protein interface (*23*). This is a similar number of intermolecular hydrogen bonds to that formed in the barnase−barstar and E9 DNase-Im9 complexes both of which show favorable enthalpy changes on complex formation (*11*, *38*). However, as compared to these other small nuclease−inhibitor complexes, and despite strong similarities in size and pI of the nucleases and inhibitor proteins involved, the E3 rRNase-Im3 complex has a much larger interface at which there is a greater degree of hydrophobic burial (*23*). In addition to this, the number of ordered water molecules at the interface is much greater, 23 for the E3 rRNase as compared to 12 for the barnase−barstar complex and five for the E9 DNase-Im9 complex (*14*). Despite these structural

Table 2: Summary of Kinetic and Equilibrium Binding Parameters for the E3 rRNase-Im3 and Colicin E3-Im3 Complexes[a]

complex	k_{on} (M^{-1} s^{-1})	k_{off} (s^{-1})	K_d (M)	ΔG (kcal mol^{-1})
E3 rRNase-Im3	$1.1(\pm0.1) \times 10^{8}$	$1.5(\pm0.1) \times 10^{-4}$	$1.4(\pm0.1) \times 10^{-12}$	−16.2
colicin E3-Im3	$5.5(\pm0.1) \times 10^{7}$	$7.6(\pm0.2) \times 10^{-7}$	$1.4(\pm0.1) \times 10^{-14}$	−18.9

[a] Values were determined in 50 mM MOPS, 200 mM NaCl, pH 7.0 at 25 °C.

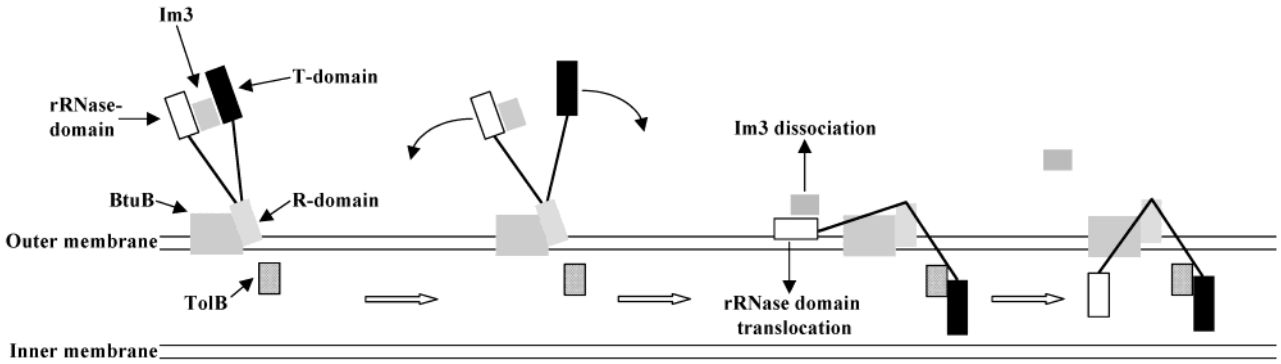

FIGURE 10: Proposed mechanism of immunity protein dissociation for the colicin E3-Im3 complex. Binding of the toxin to the outer membrane BtuB protein via the receptor binding domain triggers translocation of the T-domain into the periplasm where it forms a complex with TolB. The affinity of the toxin for the immunity protein is now reduced allowing it to dissociate from the toxin. This triggers translocation of the cytotoxic domain into the periplasm and ultimately the cytoplasm.

differences, association of E3 rRNase with Im3 shows distinct similarities to the formation of the E9 DNase-Im9 and barnase−barstar complexes, the association being both diffusion controlled and highly salt dependent. It seems likely that rapid association of the inhibitor protein is important to the efficient inhibition of these potentially toxic nucleases as this characteristic is also shared with other nuclease−inhibitor complexes such as the angiogenin−RI complex (*39*). From a kinetic standpoint, the association of E3 rRNase with Im3, which is described by a single process when monitored by stopped flow fluorescence, resembles the association of barnase and barstar (*12*) and is distinct from the association of the E9 DNase with Im9, which proceeds through two distinct, observable kinetic phases indicating a conformational change on complex formation (*11*).

Thermodynamic Consequences of Bipartite Im3 Binding. Complex formation between Im3 and colicin E3 involves two distinct interfaces with the immunity protein involving the translocation and enzymatic domains of the toxin (Figure 1b). The bulk of the free energy of complex formation is due to the formation of the cytotoxic rRNase domain−immunity protein interface (−16 kcal mol^{-1}) with additional stabilization of the complex (−3 kcal mol^{-1}) provided by the interaction of the translocation domain with Im3 (Table 2). The K_d of the colicin E3-Im3 complex was calculated as 1×10^{-14} M, very close to that of the DNase type colicin E9-Im9 complex, indicating that the evolution of high-affinity rRNase and DNase type colicin−immunity protein complexes are likely governed by similar selective pressures.

In some respects, the contribution of the translocation domain−Im3 interaction to the overall stability of the colicin E3-Im3 complex seems to be rather modest as the size of this interface is substantial at 1600 $Å^2$, representing 38% of the total loss of accessible surface area on complex formation (*24*). The resolution of the full-length colicin E3-Im3 crystal structure (3 Å) does not permit detailed analysis of the molecular interactions at this interface. It is, however, apparent that in contrast to the E3 rRNase-Im3 interface where many basic and acidic residues from E3 rRNase and Im3, respectively, are buried, there are relatively few complementary electrostatic interactions at the translocation domain−Im3 interface. In addition to this, the shape complementarity at the translocation domain−Im3 interface is poorer than that at the E3 rRNase-Im3 interface. This can be appreciated by comparing the shape complementarity index (*Sc*) for each interface as calculated by the method of Lawrence and Colman (*40*), where a value of zero indicates no complementarity and a value of one a perfect fit. Using the colicin E3-Im3 structure (PDB code 1jch), *Sc* values of 0.65 and 0.58 for the E3 rRNase-Im3 and translocation domain−Im3 interfaces, respectively, were obtained. The shape complementarity index for the enzymatic domain−Im3 interface is slightly lower than that calculated from the earlier E3 rRNase-Im3 complex structure (2.4 Å) reported by Carr et al. (*23*), where a value of 0.7 was obtained, likely reflecting the differences in structural resolution.

It is intriguing that T-domain residues that contact the immunity protein are conserved in both DNase and rRNase colicins, yet their respective immunity proteins are structurally unrelated. Wallis et al. (*11*) have shown previously that the affinity of Im9 for colicin E9 is identical to that for the isolated E9 DNase domain suggesting either that the T-domain in this complex does not contact Im9 or that, if it does, the conserved T-domain residues must be making a different (and energetically neutral) contact.

Since it is thought that only the cytotoxic domains of the enzymatic colicins translocate into the cytoplasm, both complexes studied here are likely to be physiologically relevant. The colicin E3-Im3 complex is that formed in the producing cell ($K_d = 10^{-14}$ M), and the E3 rRNase-Im3 complex represents that formed between the inhibitor protein and the colicin E3 imported into the cell from an exogenous source ($K_d = 10^{-12}$ M). Interestingly, in the case of the DNase type colicins, it has been estimated, from colicin toxicity assays against cells producing mutant immunity proteins with a range of binding affinities, that the immunity

protein must possess an affinity for the exogenous toxin of the order of 10^{-10} M in order for it to provide full biological protection (Li, Keeble, and Kleanthous, unpublished observations).

Physiological Implications. The mechanism through which the cytotoxic domains of the enzymatic colicins are able to translocate into the cytoplasm of susceptible cells is not fully understood. It is known that the colicin first anchors itself to a target cell by binding to the outer membrane BtuB receptor (*41*) and that a specific region of the colicin translocation domain (known as the TolB box) passes into the periplasm and interacts with the TolB protein (*42*, *43*). The exact role of the interaction of the toxin with TolB in translocating the cytotoxic domain is unclear as is the role of the porin OmpF that is also inferred to be involved in the translocation process (*44*).

Bipartite recognition of the immunity protein suggests a mechanism through which the immunity protein can dissociate from the toxin on binding to a target cell (Figure 10). In this mechanism, binding of the toxin to the BtuB receptor triggers translocation of some or all of the T-domain into the periplasm (a process that may involve OmpF) where it forms a complex with TolB (*42*). Contacts between the T-domain and Im3 are now lost, which weakens the interaction between toxin and immunity protein, and in particular, significantly increases the dissociation rate of the complex. This mechanism may go some way to explaining the apparent paradox that the enzymatic colicin−immunity protein complexes display high affinities and very slow dissociation rates, whereas the immunity protein is readily dissociated on binding to a target cell (*9*). For the E3 rRNase-Im3 complex, the half-lives for complex dissociation measured at 35 and 40 °C were approximately 20 and 7 min, respectively, a similar time scale to that seen for the lethal effects of the enzymatic colicins on cells in liquid culture at 37 °C (*41*, *45*). Thus, at least for colicin E3, dissociation of the immunity protein can be explained without the need to postulate any other interactions involving the colicin and target cell. However, this may not be the case for the DNase colicin E9 and its interaction with Im9 since the affinity of this complex is not influenced by the presence of the T-domain (see above), although even here the dissociation rate constant is very temperature dependent (*11*). There are also other differences between the rRNase and the DNase−immunity systems. Removal of the immunity protein from colicin E3 leads to a substantial loss of bactericidal activity of the toxin, which can be regained by reforming the complex through adding back Im3 (ref *10*, unpublished observations). This suggests a dual role for Im3 of providing both immunity to the producing cell but also stabilizing the toxin prior to cell entry, either by enhancing its resistance to proteolysis or presenting the toxin in the correct conformation for translocation. In the DNase colicin system, removal of the immunity protein does not lead to loss of bactericidal activity (*28*), further suggesting that the structural organization of the immunity protein relative to the T-domain in DNase and RNase colicins may be different.

ACKNOWLEDGMENT

We are grateful to Andrew Leech for performing the analytical ultracentrifugation experiments, Chris Penfold for assistance during the early part of this work, Maria Mate Perez for help with the construction of Figure 1, and members of the CK lab for helpful discussion.

REFERENCES

1. Parret, A. H. A., and De Mott, R. (2002) Bacteria killing their own kind: novel bacteriocins of Pseudomonas and other γ-proteobacteria, *Trends Microbiol. 10*, 107−12.
2. Sharma, S., Waterfield, N., Bowen, D., Rocheleau, T., Holland, L., James, R., and French-Constant, R. (2002) The lumicins: novel bacteriocins from *Photorhabdus luminescens* with similarity to the uropathogenic-specific protein (USP) from uropathogenic, *Escherichia coli*, *FEMS Microbiol. Lett. 214*, 241−9.
3. Pommer, A. J., Cal, S., Keeble, A. H., Walker, D., Evens, S. J., Kuhlmann, U. C., Cooper, A., Connolly, B. A., Hemmings, A. M., Moore, G. R., James, R., and Kleanthous, C. (2001) Mechanism and cleavage specificity of the H−N−H endonuclease colicin E9, *J. Mol. Biol. 314*, 735−49.
4. Tomita, K., Ogawa, T., Uozumi, K., Watanabe, K., and Masaki, H. (2000) A cytotoxic ribonuclease which specifically cleaves four isoaccepting arganine tRNAs at their anticodon loops, *Proc. Natl. Acad. Sci. U.S.A. 97*, 8278−83.
5. Bowman, C. M., Dahlberg, J. E., Ikemura, T., Konisky, J., and Nomura, M. (1971) Specific inactivation of 16S ribosomal RNA induced by colicin E3 in vivo, *Proc. Natl. Acad. Sci. U.S.A. 68*, 964−8.
6. Cramer, W. A., Cohen, F. S., Merrill, A. R., and Song, H. Y. (1990) Structure and dynamics of the colicin E1 channel, *Mol. Microbiol. 4*, 519−26.
7. Harkness, R. E., and Braun, V. (1989) Colicin M inhibits peptidoglycan biosynthesis by interfering with lipid carrier recycling, *J. Biol. Chem. 15*, 6177−82.
8. Kleanthous, C., Hemmings, A. M., Moore, G. R., and James, R. (1998) Immunity proteins and their specificity for endonuclease colicins: telling right from wrong in protein−protein recognition, *Mol. Microbiol. 28*, 227−33.
9. Krone, W. J., de Vries, P., Koningstein, G., de Jonge, A. J., de Graaf, F. K., and Oudega, B. (1986) Uptake of cloacin DF13 by susceptible cells: removal of immunity protein and fragmentation of cloacin molecules, *J. Bacteriol. 166*, 260−268.
10. Ohno, S., Ohno-Iwashita, Y., Suzuki, K., and Imahori, K. (1977) Purification and characterization of active component and active fragment of colicin E3, *J. Biochem. (Tokyo) 82*, 1045−53.
11. Wallis, R., Moore, G. R., James, R., and Kleanthous, C. (1995) Protein−protein interactions in colicin E9 DNase−immunity protein complexes. 1. Diffusion-controlled association and femtomolar binding for the cognate complex, *Biochemistry 34*, 13743−50.
12. Schreiber, G., and Fersht, A. R. (1993) Interaction of barnase with its polypeptide inhibitor barstar studied by protein engineering, *Biochemistry 32*, 5145−50.
13. Lee, F. S., Shapiro, R., and Vallee, B. L. (1989) Tight-binding inhibition of angiogenin and ribonuclease A by placental ribonuclease inhibitor, *Biochemistry 28*, 225−30.
14. Kleanthous, C., and Walker, D. (2001) Immunity proteins: enzyme inhibitors that avoid the active site, *Trends Biochem. Sci. 10*, 624−31.
15. Buckle, A. M., Schreiber, G., and Fersht, A. R. (1994) Protein−protein recognition: crystal structural analysis of a barnase−barstar complex at 2.0-Å resolution, *Biochemistry 33*, 8878−89.
16. Buckle, A. M., and Fersht, A. R. (1994) Subsite binding in an RNase: structure of a barnase−tetranucleotide complex at 1.76-Å resolution, *Biochemistry 33*, 1644−53.
17. Putnam, C. D., Shroyer, M. J., Lundquist, A. J., Mol, C. D., Arvai, A. S., Mosbaugh, D. W., and Tainer, J. A. (1999) Protein mimicry of DNA from crystal structures of the uracil−DNA glycosylase inhibitor protein and its complex with *Escherichia coli* uracil−DNA glycosylase, *J. Mol. Biol. 287*, 331−46.
18. Parikh, S. S., Mol, C. D., Slupphaug, G., Bharati, S., Krokan, H. E., and Tainer, J. A. (1998) Base excision repair initiation revealed by crystal structures and binding kinetics of human uracil−DNA glycosylase with DNA, *EMBO J. 17*, 5214−26.
19. Noeske-Jungblut, C., Haendler, B., Donner, P., Alagon, A., Possani, L., and Schleuning, W. D. (1995) Triabin, a highly potent exosite inhibitor of thrombin, *J. Biol. Chem. 270*, 28629−34.
20. Wallis, R., Leung, K. Y., Pommer, A. J., Videler, H., Moore, G. R., James, R., and Kleanthous, C. (1995) Protein−protein interac-

tions in colicin E9 DNase−immunity protein complexes. 2. Cognate and noncognate interactions that span the millimolar to femtomolar affinity range, *Biochemistry 34*, 13751−9.
21. Senior, B. W., and Holland, I. B. (1971) Effect of colicin E3 upon the 30S ribosomal subunit of *Escherichia coli*, *Proc. Natl. Acad. Sci. U.S.A. 68*, 959−63.
22. Cate, J. H., Yusupov, M. M., Yusupova, G. Z., Earnest, T. N., and Noller, H. F. (1999) X-ray crystal structures of 70S ribosome functional complexes, *Science 285*, 2095−104.
23. Carr, S., Walker, D., James, R., Kleanthous, C., and Hemmings, A. M. (2000) Inhibition of a ribosome-inactivating ribonuclease: the crystal structure of the cytotoxic domain of colicin E3 in complex with its immunity protein, *Struct. Fold. Des. 8*, 949−60.
24. Soelaiman, S., Jakes, K., Wu, N., Li, C., and Shoham, M. (2001) Crystal structure of colicin E3: implications for cell entry and ribosome inactivation, *Mol. Cell 8*, 1053−62.
25. Chak, K. F., and James, R. (1984) Localization and characterization of a gene on the ColE3−CA38 plasmid that confers immunity to colicin E8, *J. Gen. Microbiol. 130*, 701−10.
26. Garinot-Schneider, C., Pommer, A. J., Moore, G. R., Kleanthous, C., and James, R. (1996) Identification of putative active-site residues in the DNase domain of colicin E9 by random mutagenesis, *J. Mol. Biol. 260*, 731−42.
27. Wallis, R., Reilly, A., Barnes, K., Abell, C., Campbell, D. G., Moore, G. R., James, R., and Kleanthous, C. (1994) Tandem overproduction and characterisation of the nuclease domain of colicin E9 and its cognate inhibitor protein Im9, *Eur. J. Biochem. 220*, 447−54.
28. Wallis, R., Reilly, A., Rowe, A., Moore, G. R., James, R., and Kleanthous, C. (1992) In vivo and in vitro characterization of overproduced colicin E9 immunity protein, *Eur. J. Biochem. 207*, 687−95.
29. Levinson, B. L., Pickover, C. A., and Richards, F. M. (1983) Dimerization by colicin E3 in the absence of immunity protein, *J. Biol. Chem. 258*, 10967−72.
30. McRorie, D. K., and Voelker, P. J. (1993) *Self-associating systems in the analytical ultracentrifuge*, Beckman Instruments, Palo Alto, CA.
31. Jakes, K. S., and Zinder, N. D. (1974) Highly purified colicin E3 contains immunity protein, *Proc. Natl. Acad. Sci. U.S.A. 71*, 3380−4.
32. Fersht, A. R. (1998) *Structure and mechanism in protein science*, W. H. Freeman, New York.
33. Schreiber, G., and Fersht, A. (1996) Rapid, electrostatically assisted association of proteins, *Nature Struct. Biol. 3*, 427−431.
34. Vijayakumar, M., Wong, K. Y., Schreiber, G., Fersht, A. R., Szabo, A., and Zhou, H. X. (1998) Electrostatic enhancement of diffusion-controlled protein−protein association: comparison of theory and experiment on barnase and barstar, *J. Mol. Biol. 278*, 1015−24.
35. Gutfreund, H. (1995) *Kinetics for the life sciences*, Cambridge University Press, Cambridge.
36. Frisch, C., Fersht, A. R., and Schreiber, G. (2001) Experimental assignment of the structure of the transition state for the association of barnase and barstar, *J. Mol. Biol. 308*, 69−77.
37. Kleanthous, C., and Pommer, A. (2000) Nuclease inhibitors, in *Protein−Protein Recognition* (Kleanthous, C., Ed.) pp 280−311, Oxford University Press, Oxford.
38. Frisch, C., Schreiber, G., Johnson, C. M., and Fersht, A. R. (1997) Thermodynamics of the interaction of barnase and barstar: changes in free energy versus changes in enthalpy on mutation, *J. Mol. Biol. 267*, 696−706.
39. Lee, F. S., Auld, D. S., and Vallee, B. L. (1989) Tryptophan fluorescence as a probe of placental ribonuclease inhibitor binding to angiogenin, *Biochemistry 28*, 219−24.
40. Lawrence, M. C., and Colman, P. M. (1993) Shape complementarity at protein/protein interfaces, *J. Mol. Biol. 234*, 946−50.
41. Penfold, C. N., Garinot-Schneider, C., Hemmings, A. M., Moore, G. R., Kleanthous, C., and James, R. (2000) A 76-residue polypeptide of colicin E9 confers receptor specificity and inhibits the growth of vitamin B12-dependent *Escherichia coli* 113/3 cells, *Mol. Microbiol. 38*, 639−49.
42. Bouveret, E., Rigal, A., Lazdunski, C., and Bénédetti, H. (1997) The N-terminal domain of colicin E3 interacts with TolB which is involved in the colicin translocation step, *Mol. Microbiol. 23*, 909−20.
43. Carr, S., Penfold, C. N., Bamford, V., James, R., and Hemmings, A. M. (2000) The structure of TolB, an essential component of the tol-dependent translocation system, and its protein−protein interaction with the translocation domain of colicin E9, *Struct. Fold. Des. 8*, 57−66.
44. Benedetti, H., Frenette, M., Baty, D., Lloubes, R., Geli, V., and Lazdunski, C. (1989) Comparison of the uptake systems for the entry of various BtuB group colicins into *Escherichia coli*, *J. Gen. Microbiol. 135*, 3413−20.
45. De Graaf, F. K. (1973) Effects of cloacin DF13 on the functioning of the cytoplasmic membrane, *Antonie Van Leeuwenhoek 39*, 109−19.

BI0273720